Role of Insulin-Like Growth Factor Binding Protein-3 in the Pathogenesis of Herpes Stromal Keratitis

Pushpa Rao,[1] Pratima K. Suvas,[1] Andrew D. Jerome,[2] Jena J. Steinle,[1] and Susmit Suvas[1]

[1]Department of Ophthalmology, Visual and Anatomical Sciences, Wayne State University School of Medicine, Detroit, Michigan, United States
[2]The Ohio State University Wexner Medical Center, Columbus, Ohio, United States

Correspondence: Susmit Suvas, 7223 Scott Hall, Department of Ophthalmology, Visual and Anatomical Sciences and Department of Biochemistry, Microbiology and Immunology, Wayne State University School of Medicine, Detroit, MI, USA; ssuvas@med.wayne.edu.

Received: October 21, 2019
Accepted: December 5, 2019
Published: February 27, 2020

Citation: Rao P, Suvas PK, Jerome AD, Steinle JJ, Suvas S. Role of insulin-like growth factor binding protein-3 in the pathogenesis of herpes stromal keratitis. *Invest Ophthalmol Vis Sci.* 2020;61(2):46. https://doi.org/10.1167/iovs.61.2.46

Purpose. The goal of this study was to determine the role of insulin-like growth factor-binding protein-3 (IGFBP-3) in the pathogenesis of herpes stromal keratitis (HSK).

Methods. In an unbiased approach, a membrane-based protein array was carried out to determine the level of expression of pro- and anti-angiogenic molecules in uninfected and HSV-1 infected corneas. Quantitative RT-PCR and ELISA assays were performed to measure the amounts of IGFBP-3 at mRNA and protein levels. Confocal microscopy documented the localization of IGFBP-3 in uninfected and infected corneal tissue. Flow cytometry assay showed the frequency of immune cell types in infected corneas from C57BL/6J (B6) and IGFBP-3 knockout (IGFBP-3$^{-/-}$) mice. Slit-lamp microscopy was used to quantitate the development of opacity and neovascularization in infected corneas from both groups of mice.

Results. Quantitation of protein array dot blot showed an increased level of IGFBP-3 protein in HSV-1 infected than uninfected corneas and was confirmed with ELISA and quantitative RT-PCR assays. Cytosolic and nuclear localization of IGFBP-3 were detected in the cells of corneal epithelium, whereas scattered IGFBP-3 staining was evident in the stroma of HSK developing corneas. Increased opacity and hemangiogenesis were noted in the corneas of IGFBP-3$^{-/-}$ than B6 mice during the clinical period of HSK. Furthermore, an increased number of leukocytes comprising of neutrophils and CD4 T cells were found in HSK developing corneas of IGFBP-3$^{-/-}$ than B6 mice.

Conclusions. Our data showed that lack of IGFBP-3 exacerbates HSK, suggesting the protective effect of IGFBP-3 protein in regulating the severity of HSK.

Keywords: HSV-1, inflammation, cornea, herpes keratitis

Recurrent corneal infection with herpes simplex virus-1 (HSV-1) may cause the development of a chronic immunoinflammatory condition known as herpes stromal keratitis (HSK).[1–3] During the development of HSK, the cornea loses its clarity, becomes opaque, and gets heavily vascularized. The newly formed leaky blood vessels enter into the corneal stroma from the limbal area and travel toward the center of the cornea, thereby affecting the visual axis.[4] Also, massive infiltration of different subsets of leukocytes are reported in HSK-developing corneas.[5–7] Among them, neutrophils and T cells are the most prominent immune cell types that orchestrate damage to the corneal stroma by releasing cytokines, growth factor, and proteases.[5,8] The current management of HSK involves the use of oral antivirals and topical application of corticosteroids.[9,10] However, long-term use of corticosteroids from the recurrence of HSK, have significant side effects including the development of glaucoma, cataract, and the reactivation of latent HSV-1 infection.[11,12] Thus, a better understanding of immunoinflammatory events in HSK-developing corneas is a prerequisite for developing specific immunotherapeutic approaches to modulate the severity of HSK.

Insulin-like growth factor binding protein-3 (IGFBP-3) belongs to the family of six highly conserved proteins that are encoded by IGFBP1 to IGFBP6 genes.[13–18] These proteins are characterized by their higher affinity for insulin-like growth factors (IGFs), IGF-I and IGF-II.[13,19,20] In serum, IGFBP-3 is the most abundant IGFBP molecule and is involved in transporting IGF-I and IGF-II proteins in large complexes.[15,21] IGFBP-3 in circulation forms a 150-kDa ternary complex with IGF-I/II and acid labile subunit.[22,23] Approximately, 75% to 90% of IGF-I/II in circulation is transported with IGFBP-3, and the latter play an important role in regulating the stability and bioavailability of IGF-I molecule. In addition, IGFBP-3 is also known to act in IGF-independent mode and exhibits anti-proliferative and pro-apoptotic effects.[15,24–26] IGFBP-3 is reported to present in human corneal epithelial cells[27] and in the tears of diabetic individuals.[28,29] However, the role of IGFBP-3, if any, in regulating the pathogenesis of HSK is not known.

In the current study, we measured the amounts of IGFBP-3 protein in HSV-1-infected corneas and determined their involvement in regulating the severity of HSK lesions. Our results showed an increased level of IGFBP-3 in HSK

developing corneas. The lack of IGFBP-3 resulted in the exacerbation of HSK and was associated with an increased number of leukocytes in infected corneas of IGFBP-3$^{-/-}$ than B6 mice. Together, these results suggest the protective action of IGFBP-3 in HSK lesions. Our results are discussed to define the possible mechanisms by which IGFBP-3 exerts their protective effect in HSK lesions.

Methods

Mice

Eight- to 12-week-old C57BL/6J female (B6, stock no. 000664) mice were procured from Jackson laboratory (Bar Harbor, ME). Age-matched IGFBP3$^{-/-}$ female mice on B6 background were used for the studies described in this report. IGFBP-3$^{-/-}$ breeders were originally obtained from Dr. Pintar.[30] The colony of IGFBP-3$^{-/-}$ mice were breed and housed at the Division of Laboratory Animal Resources facility at Wayne State University School of Medicine. Functional ablation of IGFBP-3 gene was confirmed both at the protein and gene level (data not shown). All experimental procedures were performed in a class II, type 2 biosafety cabinet and were in complete agreement with the Association for Research in Vision and Ophthalmology statement for the use of animals in ophthalmic and vision research. All animal experiments were carried out in accordance with the rules and regulations of The Institutional Animal Care and Use Committee of Wayne State University.

Virus and Corneal HSV-1 Infection

HSV-1 RE Tumpey strain used in the current study was propagated on monolayer of Vero cells (American Type Culture Collection, Manassas, VA; CCL81) as described previously.[31] Primary ocular HSV-1 infection in B6 and IGFBP-3$^{-/-}$ groups of mice was performed by first, anesthetizing the mice (20 g body weight) via intraperitoneal injection of ketamine HCl (33 mg/kg/body weight) and Xylazine HCl (20 mg/kg/body weight) solution. The effect of anesthesia was determined with toe pinch reflex. The anesthetized mouse corneas were scarified using a 27-G needle and a dose of 1×10^5 or 1×10^4 plaque-forming unit (PFU) of virus in 3µl of 1xPBS was topically applied to the scarified corneas followed by gentle massage of the eyelids.

Mouse Angiogenesis Protein Array Analysis

Angiogenesis array was conducted as per manufacturer instructions using mouse angiogenesis array kit, (cat# ARY015 R&D systems). Briefly, uninfected and eyes infected with HSV-1 (1×10^5 PFU/eye) were enucleated from B6 mice at 5, 10, and 15 days postinfection. Corneas were dissected from the respective eyeballs under the stereomicroscope and transferred into 250 µL of PBS containing protease inhibitor cocktail (Sigma-Aldrich Co.) and saved immediately at −80°C. Individual cornea samples were sonicated using Sonic Dismembrator ultrasonic processor at 50% amplitude with a cycle of 15-second pulse, followed by 1 minute resting on ice. A total of six cycles were given to each cornea. Tissue lysates (sonicated samples) were centrifuged at 4°C at 15,000 rpm for 10 minutes. The supernatant was collected and the amount of protein in each sample was estimated using BCA protein assay kit (cat# 23225, Thermo Scientific). A total of 200 µg of protein from tissue lysates from each group was used for angiogenesis array analysis as per the manufacturer's instructions. The membranes were scanned using FluorChem E Imager system. Positive signals on the membranes were quantified using Image Studio Lite Version 4.0.

Immunofluorescence Staining

Immunofluorescence to detect IGFBP-3 protein was carried out on 8-µm-thick frozen corneal sections. The frozen corneal sections from uninfected B6 and IGFBP-3$^{-/-}$ mice eyes and from 4-, 10-, and 14- day postinfected B6 mouse eyes were fixed in 2% paraformaldehyde for 30 minutes at room temperature. Sections were washed three times in 1X PBS followed by blocking with blocking buffer (1X PBS + 3% BSA + 0.3% Triton-X-100) for 2 hours at room temperature. After 2 hours, sections were incubated with primary unconjugated anti-IGFBP-3 antibody overnight at 4°C. The next day, slides were washed three times with 1X PBS + 0.3% Triton-X-100 solution and then incubated at room temperature for 2 hours with Alexa Fluor 488 conjugated secondary antibody. Next, the slides were washed three times with 1X PBS + 0.3% Triton-X-100 solution and later mounted with DAPI containing mounting medium (Vector Laboratories, CA). Images were acquired using a Leica True Confocal Scanner SP8 confocal microscope. Antibody dilutions were made in dilution buffer (1X PBS + 1% BSA + 0.3% Triton-X-100). Sources and dilutions of antibodies are provided in the Table.

ELISA to Determine the Amount of IGFBP-3 in the Serum and Cornea of B6 Mice

ELISA was performed to determine the amount of IGFBP-3 in the serum of uninfected and HSV-1 infected B6 mice at 4, 5, and 10 days post-HSV-1 infection. Diluted serum samples were used to assay for IGFBP-3 protein level using mouse IGFBP-3 DuoSet ELISA kit (DY775, R&D Systems, MN). On the other hand, HSV-1-infected cornea samples obtained at 5 and 15days postinfection from B6 mice were sonicated followed by centrifugation at 3000 rpm for 10 minutes at 4°C.

The supernatant was collected and assayed for IGFBP-3 using DuoSet ELISA kit as per the manufacturer's instruction. Sample absorbance was measured at 410 nm (A_{410}) on a microplate reader (SpectraMax M5 multimode microplate reader) and the results were expressed as picograms/milliliter.

Quantitative RT-PCR assay

Uninfected and HSV-1 infected eyes from B6 mice were collected in RNAlater at 5 and 10 days postinfection and corneas were excised under stereomicroscope. Individual cornea samples were processed to extract RNA using RNA STAT-60 solution (Tel-Test, Friendswood, TX) according to the manufacturer's instructions. Purified RNA was quantified using the NanoDrop ND -1000 spectrophotometer (Thermo Fisher Scientific, Waltham, MA). One microgram of RNA was reverse transcribed using iScript cDNA synthesis kit (Bio-Rad) to generate the cDNA template for quantitative RT-PCR (qRT-PCR) assay. A 1-µL aliquot of cDNA was used for qRT-PCR reaction with SYBR green/fluorescein PCR master mix (Bio-Rad Laboratories, Richmond, CA). Opti-

Investigative Ophthalmology & Visual Science

Table. Antibodies for Immunofluorescence and Flow Cytometry.

Antibody	Clone	Fluorochrome	Dilution	Catalog No.
IGFBP-3	Polyclonal	Unconjugated	1:50	Santacruz SC9028
Donkey anti-rabbit	Polyclonal	Alexa 488	1:200	Molecular Probes A21206
CD4	RM4-5	BV605	1:100	BD Biosciences, 563151
CD11b	M1/70	PerCp-Cy5.5	1:100	BD Biosciences, 550993
CD45	30F-11	PE-Cy7	1:100	BD Biosciences, 552848
Ly6G	1A8	Alexa 700	1:100	BD Biosciences, 561236

mal conditions for qRT-PCR assay were set as per the recommendations of Bio-Rad. qRT-PCR assay was carried out using CFX-Connect Real-time PCR Detection System (Bio-Rad Laboratories). The fold differences in gene expression was calculated after normalization with housekeeping GAPDH gene and represented as relative gene expression ± SEM using the $2^{-\Delta\Delta CT}$ method of calculation.

Clinical Scoring of HSK

For clinical scoring of HSK, B6 and IGFBP3$^{-/-}$ mice were infected with 1×10^4 PFU of HSV-1 RE (Tumpey) strain and the extent of corneal opacity and angiogenesis was measured by a masked observer 7, 10, and 12 days postinfection using a hand-held slit-lamp biomicroscope (Kowa, Nagoya, Japan) as described earlier.[32] Briefly, a standard scale for corneal opacity, ranging from 0 to 5 was used, and the extent of corneal hemangiogenesis was determined by measuring the centripetal growth of newly formed blood vessels in each quadrant of infected cornea.

Cell Surface Staining by Flow Cytometry

HSV-1-infected eyes from B6 and IGFBP3$^{-/-}$ mice were enucleated at 13 days postinfection and collected in the ice-cold RPMI 1640 medium with antibiotics. The corneas were dissected by using the curved fine forceps (Miltex, York, PA) under the dissecting microscope to separate out the underlying lens, ciliary body, iris, and the scleral tissue. The individual cornea sample was suspended in 250 µL of RPMI 1640, and 20 µL of Liberase TL (2.5 mg/mL) was added followed by incubation at 37°C for 45 minutes on a tissue disruptor. At the end of incubation, the tissue was triturated using 3-mL syringe plunger and passed through a 70-µm cell strainer. This was followed by pelleting down the cells at 315*g* for 8 minutes in a refrigerated centrifuge. The single-cell suspensions from the individual corneas were washed with FACS buffer (PBS + 2% FBS + 0.1% sodium azide). Next, to block the Fc receptors, cornea samples were incubated on ice with anti-mouse CD16/32 Ab for 30 minutes followed by staining with cell-surface antibodies. At the end of the cell-surface staining, samples were fixed in 1% paraformaldehyde and samples were acquired on LSRFortessa flow cytometer. Data were analyzed using FlowJo software. Sources and dilutions of Abs are provided in the Table.

Statistical Analysis

Statistical analysis was calculated using GraphPad Prism software (San Diego, CA). Significance was determined by unpaired two-tailed parametric *t* test (with Welch's correction) or nonparametric Mann-Whitney *U* test. One-way ANOVA was used to determine statistically significant differences when comparing the results of more than two independent groups. Differences were considered statistically significant as follows: $^*P \leq 0.05$, $^{**}P \leq 0.01$, $^{***}P \leq 0.001$, and $^{****}P \leq 0.0001$.

Results

Increased Level of IGFBP-3 Protein in HSV-1-Infected Cornea

The development of HSK is associated with the formation of new leaky blood vessels in HSV-1-infected corneas.[4] In an unbiased approach, a membrane-based protein angiogenesis array was carried out on the tissue lysates obtained from uninfected and HSV-1 infected corneas at 5, 10, and 15 days postinfection, as described in the Methods. The quantification of the signal intensity of protein molecules on the membrane was performed using Image Studio Lite Version 4.0 software. Our results showed that in comparison to uninfected corneal tissue, HSV-1-infected corneas had an increased level of several angiogenesis regulating molecules such as osteopontin, FGF-2, platelet factor 4, and IGFBP-3 (Fig. 1). Quantification of signal intensity showed that in comparison to uninfected cornea, HSK developing corneas had more than 40-fold increase in signal intensity of IGFBP-3 protein at 10 and 15 days postinfection. Similarly, about fourfold increase in the signal intensity of MMP-3 matrix metalloproteinase (MMP) protein was detected in HSK developing corneas at 10 and 15 days postinfection. Our results also showed about 50% decrease in the level of tissue inhibitor of metalloproteinase-1 (TIMP-1) molecule in HSK corneas at 15 days postinfection, when compared with HSK developing corneas at 10 days postinfection (Fig. 1C). Because of our specific interest in understanding the role of IGFBP-3 in HSK-developing corneas, we quantified the level of IGFBP-3 protein, using ELISA assay, in HSV-1-infected corneas at 5 and 15 days postinfection. We chose these two time-points because in the mouse model, HSK is divided into preclinical (days 1-6 postinfection) and clinical disease period (days 7-18 postinfection).[33] Our results showed a significant increase in the protein level of IGFBP-3 in the corneas with HSK during clinical disease period (Fig. 1E).

Localization of IGFBP-3 in the Corneal Epithelium and Stroma of HSK Developing Corneas

Of the IGFBPs, IGFBP-3 protein is the most abundant IGFBP molecule in the peripheral circulation, which carries more than 75% of serum IGF-I and IGF-II in large complexes.[15,18] To ascertain if an increased level of IGFBP-3 in HSV-1-infected cornea is the outcome of reduced amounts of IGFBP-3 protein in circulation, we next measured the level of IGFBP-3 protein in the serum of uninfected and HSV-1-infected mice at different day postcorneal infection. As shown in Figure 2A, a significant decrease in the amount

Investigative Ophthalmology & Visual Science

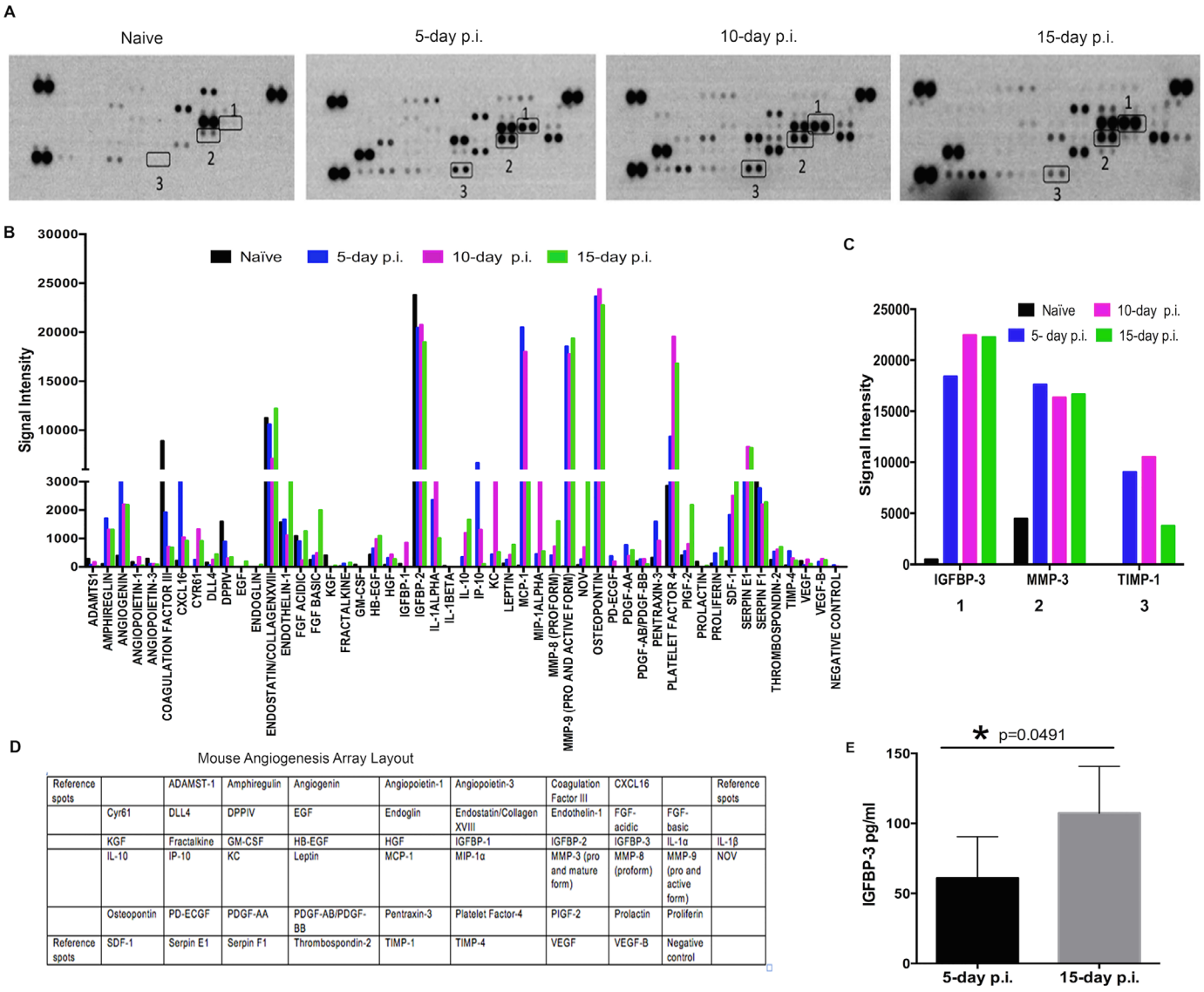

Reference spots		ADAMST-1	Amphiregulin	Angiogenin	Angiopoietin-1	Angiopoietin-3	Coagulation Factor III	CXCL16		Reference spots
	Cyr61	DLL4	DPPIV	EGF	Endoglin	Endostatin/Collagen XVIII	Endothelin-1	FGF-acidic	FGF-basic	
	KGF	Fractalkine	GM-CSF	HB-EGF	HGF	IGFBP-1	IGFBP-2	IGFBP-3	IL-1α	IL-1β
	IL-10	IP-10	KC	Leptin	MCP-1	MIP-1α	MMP-3 (pro and mature form)	MMP-8 (proform)	MMP-9 (pro and active form)	NOV
	Osteopontin	PD-ECGF	PDGF-AA	PDGF-AB/PDGF-BB	Pentraxin-3	Platelet Factor-4	PIGF-2	Prolactin	Proliferin	
Reference spots	SDF-1	Serpin E1	Serpin F1	Thrombospondin-2	TIMP-1	TIMP-4	VEGF	VEGF-B	Negative control	

Figure 1. An increased amount of IGFBP-3 protein in the lysates of HSV-1-infected corneas than uninfected corneas. (**A**) Angiogenic array blots were incubated with equivalent amount of proteins obtained from the lysates of uninfected (naive) corneas and HSV-1-infected corneas at 5, 10, and 15 days postinfection (p.i.). Array blots are showing the intensity of angiogenic molecules from uninfected and HSV-1-infected cornea samples. The numbers 1, 2, and 3 in the array blots denote IGFBP-3, MMP-3, and TIMP-1 protein molecules, respectively. (**B**) Bar diagram denotes the quantification of signal intensity of different angiogenic molecules from uninfected and HSV-1-infected cornea samples using Image Studio Lite Version 4.0 software. (**C**) Average signal intensity of IGFBP-3, MMP-3, and TIMP-1 molecules in uninfected and HSV-1-infected corneal lysates is shown in the bar graph. (**D**) Mouse angiogenesis array layout showing the position of different angiogenic molecules on membrane used for array blots. (**E**) Bar graph denotes IGFBP-3 protein level in the lysates of infected corneas at 5 and 15 days p.i. as determined by ELISA assay (n = 5 corneas at each time-point). *P* value was calculated using unpaired two-tailed Student *t*-test with Welch correction.

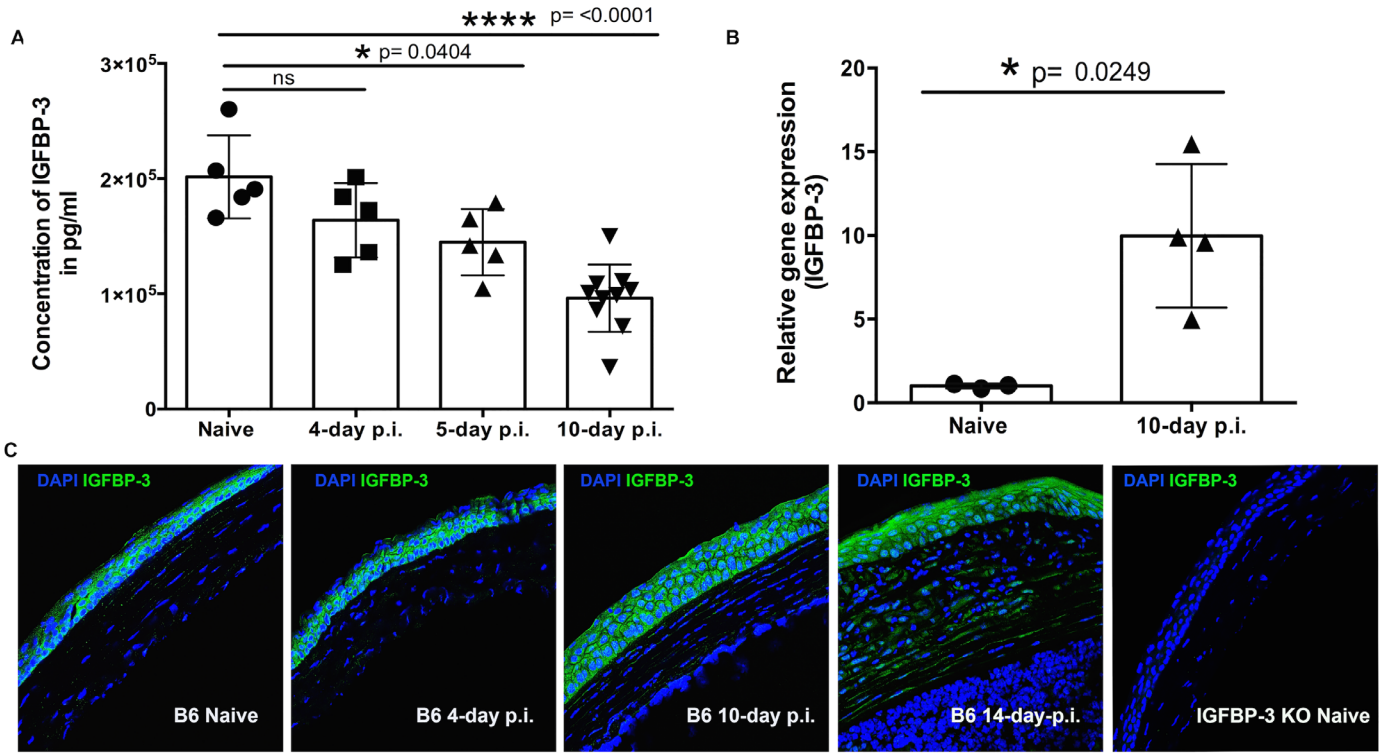

Figure 2. Reduced level of IGFBP-3 protein in circulation but an increased expression of IGFBP-3 in corneas of HSV-1-infected mice during clinical disease period of HSK. (**A**) Bar graph denotes the amount of IGFBP-3 in the serum of naive (uninfected) and HSV-1-infected mice at different day postinfection (p.i.). Each symbol in the graph represents an individual mouse. One-way ANOVA test was carried out to determine the statistical significance. (**B**) Scatter plot shows the mRNA level of IGFBP-3 in naive (uninfected) and infected cornea at 10-day p.i. Each symbol in graph denotes an individual cornea. Two-tailed Student *t*-test with Welch's correction was performed to determine the statistical significance (**C**) Representative frozen corneal sections are demonstrating IGFBP-3 staining in naive (uninfected) cornea, infected corneas at 4, 10, and 14 days p.i., and in naive IGFBP-3$^{-/-}$ cornea. IGFBP-3 (green) and DAPI nuclear staining (blue) in the corneal sections. Magnification 40× for corneal images.

of IGFBP-3 protein was noted in the serum of infected mice at 5 and 10 days postinfection when compared with serum of uninfected mice. The decrease in serum level of IGFBP-3 protein at 5 and 10 days postinfection was associated with an increased amount of IGFBP-3 protein in HSV-1-infected cornea as evident from the protein array data shown in Figure 1, suggesting a possibility of IGFBP-3 influx in inflamed cornea from the peripheral circulation. However, IGFBP-3 is also reported to express in the corneal epithelial cells,[27] and an increased expression of IGFBP-3 in inflamed cornea could also contribute to the higher level of IGFBP-3 that is detected in HSK-developing corneas. To measure the gene expression of IGFBP-3 molecule, qRT-PCR assay was carried out on uninfected and HSV-1-infected corneas. Our results showed that in comparison to uninfected corneas, HSV-1-infected corneas at 10 days postinfection displayed significantly increased level of IGFBP-3 mRNA (Fig. 2B). When present inside a cell, IGFBP-3 protein is known to interact with cytosolic proteins and get transported to the nucleus for exerting their functional activity.[24] The immunofluorescence staining of IGFBP-3 in the frozen corneal sections of HSV-1-infected corneas showed the cytosolic accumulation and nuclear localization of IGFBP-3 in epithelial cells of infected corneas (Fig. 2C). Moreover, scattered IGFBP-3 staining was also evident in the corneal stroma of eyes with HSK lesions. Together, our results showed the presence of IGFBP-3 protein in the epithelium and stroma of HSK developing corneas.

Lack of IGFBP-3 Exacerbates the Severity of HSK Lesions

Next, to ascertain if IGFBP-3 molecule could play a role in the development of HSK lesions, we performed the corneal HSV-1 infection in B6 and IGFBP-$3^{-/-}$ mice. The knockout phenotype of IGFBP-$3^{-/-}$ mice was confirmed both at the DNA and protein level (data not shown). Both groups of mice were infected with a low dose (1×10^4 p.f.u.) of HSV-1. The development of corneal opacity and hemangiogenesis was measured in both groups of mice in a masked manner using hand-held slit-lamp microscope at different time-points postinfection. The representative HSK-developing eye images from both groups of infected mice and the clinical scoring clearly showed the significantly increased scoring of the corneal opacity and hemangiogenesis in IGFBP-$3^{-/-}$ mice at 10 and 12 days postinfection in comparison to virus-infected B6 mice (Fig. 3A and B). The incidence of corneal opacity was also much higher in IGFBP-$3^{-/-}$ than B6 mice when measured at 12 days postinfection (Fig. 3C). Collectively, our results showed exacerbation of HSK lesions in IGFBP-$3^{-/-}$ mice.

Increased Number of CD4 T Cells and Neutrophils in HSK-Developing Corneas of IGFBP-$3^{-/-}$ Mice

CD4 T cells and neutrophils are the major players in orchestrating the damage to HSV-infected corneas and are reported to present in the corneas with HSK lesions.[5,8] To ascertain whether lack of IGFBP-3 affects the number of infiltrating CD4 T cells and neutrophils in HSK developing corneas, corneal HSV-1 infection was carried out in B6 and IGFBP-$3^{-/-}$ mice as described in the Methods. Mice from both groups were euthanized 13 days postinfection and the corneas were excised under stereomicroscope. Single

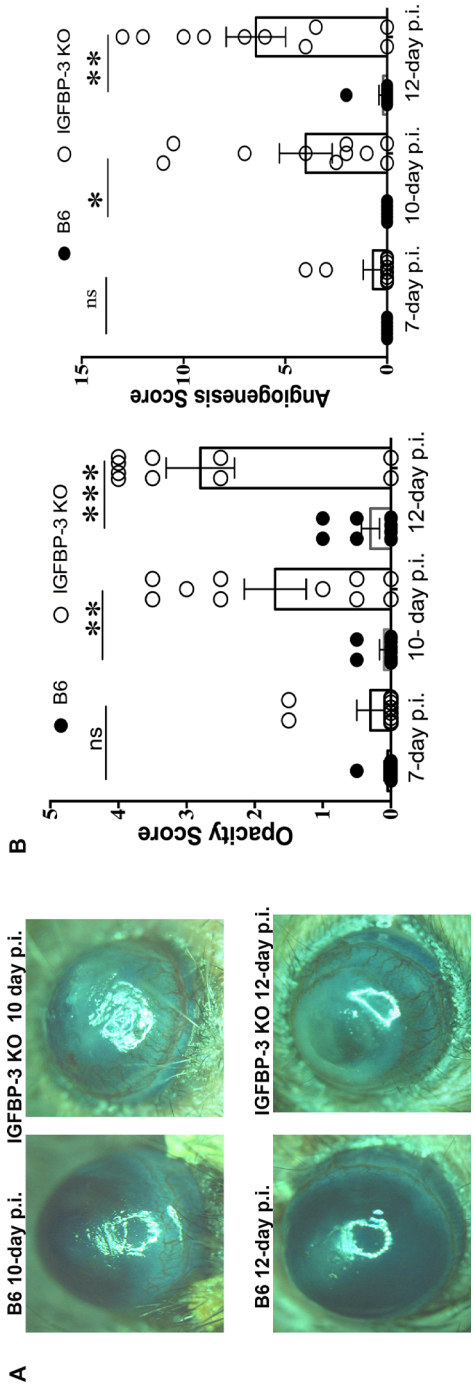

Figure 3. Exacerbation of HSK lesions in the corneas of IGFBP-$3^{-/-}$ than B6 mice. (**A**) Representative eye images are denoting the severity of corneal opacity and hemangiogenesis in infected corneas from IGFBP-$3^{-/-}$ and B6 mice at 10 and 12 days postinfection (p.i.). (**B**) Scatterplots with bar diagram are denoting the corneal opacity and hemangiogenesis grading measured using silt-lamp microscope for individual corneas from B6 and IGFBP-$3^{-/-}$ mice at 7, 10, and 12 days p.i. Unpaired parametric two-tailed *t*-test with Welch correction was used to determine the statistical significance of the data presented in the graph.

cell preparation of the corneas was carried out for flow cytometry studies as described in the Methods. Samples were acquired on LSRFortessa flow cytometer and the data was analyzed using FlowJo software. Representative FACS plots shown in Figure 4 document the gating strategy used on the corneal samples from both groups of mice. Our results showed the significant increase in the frequency and absolute number of $CD45^+$ leukocytes in the infected corneas from IGFBP-$3^{-/-}$ than B6 mice 13 days postinfection. Further analysis of leukocytic subpopulation showed higher frequency of neutrophils and an increased number of neutrophils and CD4 T cells in HSV-1-infected corneas from IGFBP-$3^{-/-}$ mice when compared with control infected B6 mice. Together, our results suggest that the increased number of CD4 T cells and neutrophils in infected corneas could exacerbate the severity of HSK in IGFBP-$3^{-/-}$ mice.

Discussion

HSK is a chronic inflammatory condition that develops in response to recurrent corneal infection with HSV-1. The hallmark of HSK is neovascularization, lymphangiogenesis, and the infiltration of neutrophils and CD4 T cells in inflamed corneal tissue.[1,4,34] A better understanding of molecular events that regulate these pathological processes is essential to develop new approaches to manage the severity of HSK. In this study, we determined the role of IGFBP-3 protein in regulating the pathogenesis of HSK. Our results showed an increased amount of IGFBP-3 protein in HSK developing corneas. The functional efficacy of IGFBP-3 in regulating the severity of HSK was determined using IGFBP-$3^{-/-}$ mice. The latter exhibited more severe hemangiogenesis, corneal opacity, and an increased number of CD4 T cells and neutrophils in HSV-1-infected corneas. Together, our results showed the protective effect of IGFBP-3 during the development of HSK.

IGFBP-3 is the major carrier protein for IGF molecules in the circulation and regulates the bioavailability of IGF-I to the extravascular compartment. Most of the circulating IGFBP-3 originates in the liver and their expression could be regulated by growth hormone because of the presence of a growth hormone-response element in IGFBP-3 gene.[35,36] Our results showed about 50% reduction in the serum level of IGFBP-3 protein in HSV-1 infected mice during clinical disease period when compared to the serum from uninfected mice. The reduction in the amounts of circulatory IGFBP-3 protein in HSK developing mice could either be due to reduced synthesis of IGFBP-3 in the liver or an increased proteolysis of IGFBP-3 in the serum.[37,38] IGFBP-3 can be cleaved by serine proteases, cathepsins, and MMPs.[39] The reduced level of circulatory IGFBP-3 protein during clinical disease period could also be due to the vascular leakage of IGFBP-3 protein complex from newly formed leaky blood vessels into HSK developing corneas. In fact, our results did show the elevated levels of IGFBP-3 protein, and scattered IGFBP-3 staining in the stroma of HSK developing corneas during clinical disease period.

Higher amounts of IGFBP-3 in HSK developing cornea could also be due to an increased expression of IGFBP-3 gene in the cells of the corneal tissue. IGFBP-3 is reported to express in corneal epithelial cells.[27] Our results showed an upregulation of IGFBP-3 mRNA expression in HSV-1-infected cornea during clinical disease period. Several factors such as TGF-β1, IGF-I, retinoic acid, TNF-α, and hypoxia are known to upregulate IGFBP-3 mRNA expression.[40–42] We recently showed the development of hypoxia in HSK-developing corneas,[43] suggesting a possibility that hypoxia might upregulate the expression of IGFBP-3 in HSK lesions. Once expressed, IGFBP-3 protein is secreted out of the cell but can be taken up in an autocrine or paracrine action through a variety of endocytic mechanisms involving caveolin-1 and clathrin-coated pits.[44,45] After the uptake, IGFBP-3 can shuttle between nucleus and cytosol and regulates the cellular apoptosis.[44,46] Specific phosphorylation of IGFBP-3 protein is considered critical for the induction of apoptosis.[47,48] Even though our confocal results showed cytosolic accumulation and the nuclear localization of IGFBP-3 protein in the corneal epithelial cells of HSK developing corneas, it did not specify if IGFBP-3 protein is phosphorylated and could cause the apoptosis of corneal epithelial cells in HSK developing eyes. It is also possible that IGFBP-3 in the corneal epithelial cells, during the development of HSK, might exerts anti-apoptotic effect as reported in endothelial cells primarily through activation of sphingosine kinase and an increased expression of sphingosine kinase 1.[49] In addition to trafficking inside the cell, IGFBP-3 can also bind to cell membrane bound receptor such as type V TGF-beta receptor (TbetaR-V) also known as low-density lipoprotein-related protein 1.[50] IGFBP-3/TbetaR-V receptor complex in association with TGF-β1 can deliver inhibitory signal and causes the growth inhibition of the cell.[50] It will be interesting to determine if corneal epithelial cells, during the development of HSK, express lipoprotein-related protein 1 and the latter regulates IGFBP-3 mediated growth inhibitory signal in the corneal epithelium. Increased expression of IGFBP-3 protein in the corneal epithelium may play an important role in regulating HSV-1 load in the infected corneas. IGFBP-3 in the IGF independent manner is reported to induce the cellular senescence,[51] and the latter is shown to reduce the viral load.[52] Besides, IGFBP-3 also regulates IGF-1R mediated signaling in macrophages,[53] and the latter immune cell type is involved in regulating the establishment of HSV-1 latency in the trigeminal ganglia.[7,54] Thus, IGFBP-3 in an IGF-dependent or independent manner may participate in regulating viral load in the cornea and trigeminal ganglia of HSV-1 infected mice.

Depending upon the microenvironment and cellular context, IGFBP-3 can either have a protective or damaging effect in an ongoing inflammation. IGFBP-3 has been shown to regulate the pathophysiology of several human diseases such as cancer, diabetes, and malnutrition.[25] The anti-angiogenic property of IGFBP-3 is reported in prostate cancer and head and neck squamous cell carcinoma.[55–57] On the other hand, overexpression of IGFBP-3 in retinal endothelium is shown to restore vascular integrity in Diabetic retinopathy.[58,59] Our results are in agreement with the anti-angiogenic effects of IGFBP-3 in an inflammatory setting, as the absence of IGFBP-3 resulted in the exacerbation of hemangiogenesis in HSK developing corneas. IGFBP-3 is reported to inhibit hemangiogenesis in IGF-independent and IGF-dependent fashion.[55,56,60] Therefore, enhanced neovascularization detected in HSK developing corneas of IGFBP-$3^{-/-}$ mice could be the outcome of IGF-dependent or independent events. In addition to an increased hemangiogenesis, our results also showed an increased number of neutrophils and CD4 T cells in HSK developing corneas of IGFBP-$3^{-/-}$ mice. Lack of IGFBP-3 is expected to increase the bioavailability of IGF-1 molecule for IGF-1R-expressing leukocytes. In B6 mice, IGF-1R signaling in leukocytes can occur either in the circulation when

Investigative Ophthalmology & Visual Science

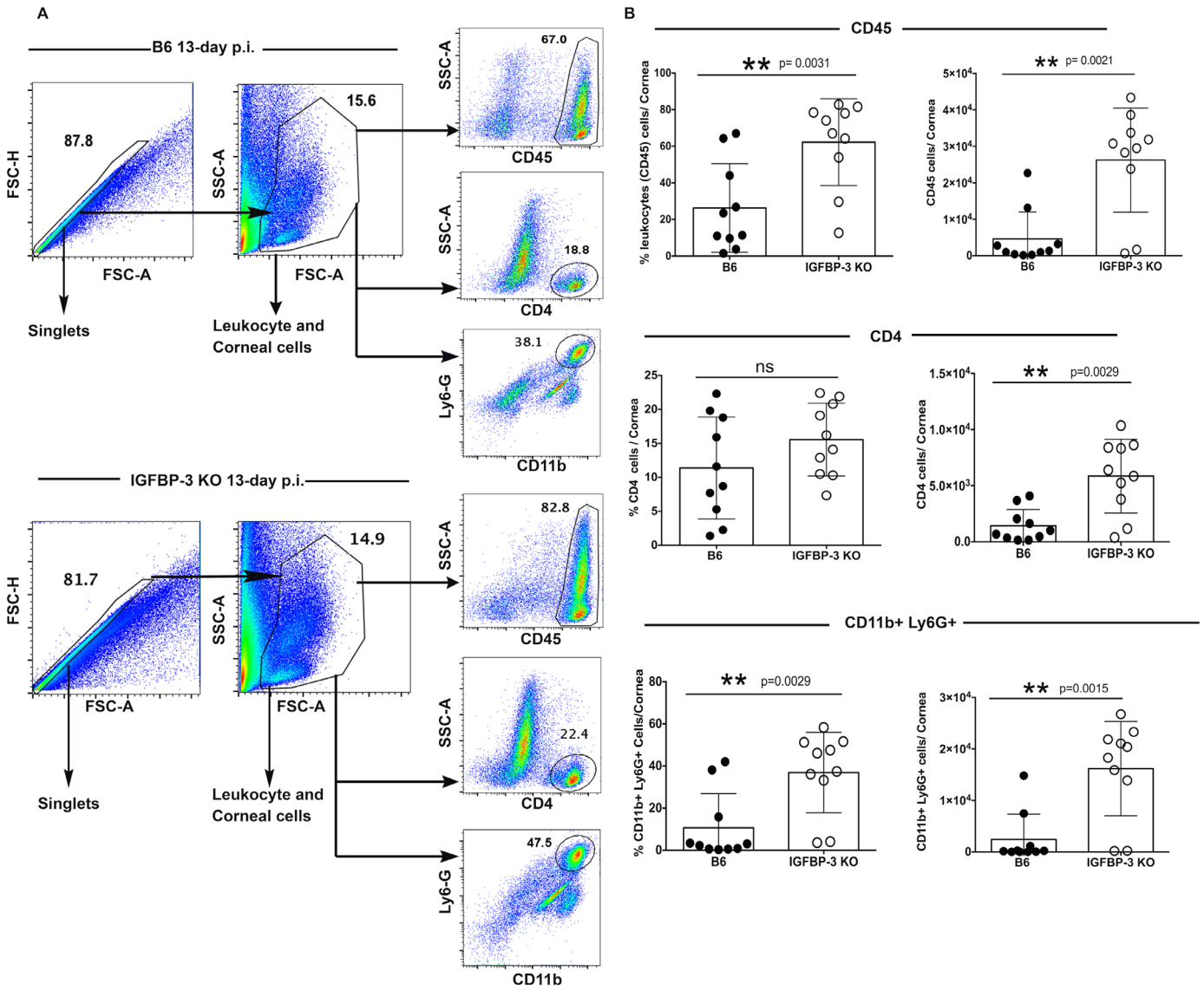

Figure 4. Increased number of neutrophils and CD4 T cells in HSK-developing corneas of IGFBP-3$^{-/-}$ than B6 mice. (**A**) Representative FACS plots are denoting the gating strategy used to determine the cell populations of singlets, leukocytes, neutrophils, and CD4 T cells in HSK-developing corneas from IGFBP-3$^{-/-}$ and B6 mice at 13 days postinfection (p.i.). (**B**) Bar diagram with scatter plots are denoting the frequency and absolute numbers of CD4 T cells and neutrophils in HSK developing corneas from both groups of mice at 13 days p.i. Each symbol in the graph represents the frequency and absolute number of immune cells in an individual cornea from each group of mice. Unpaired nonparametric Mann-Whitney test was carried out to determine the statistical significance of the data presented in the graphs.

IGFBP-3 level decreases in the peripheral blood of HSV-1-infected B6 mice (Fig. 2) or in the HSK lesions due to the proteolysis of IGFBP-3 by MMPs. IGF-1 has been shown to increase the survival of human granulocytes,[61,62] and is reported to potentiate the effector function of neutrophils.[63] Similarly, IGF-1R signaling is also reported to enhance the survival of activated T cells.[64,65] Thus, the increased number of neutrophils and CD4 T cells detected in HSK developing corneas of IGFBP-3$^{-/-}$ mice can be the direct outcome of IGF-1R mediated signaling on these immune cell subsets.

Together, our results suggested the anti-inflammatory role of IGFBP-3 in HSK setting as their absence resulted in the exacerbation of HSK lesions. In fact, anti-inflammatory role of IGFBP-3 has been reported in other inflammatory conditions.[66] Therefore, increasing the IGFBP-3 protein level in HSV-1-infected cornea is anticipated to alleviate the severity of HSK lesions.

Acknowledgments

The authors thank Bala Bharathi Burugula and Nicholas Gregory Ciavattone for technical assistance in performing protein array blot assay.

Supported by National Eye Institute Grant R01EY029690 (SS), R01EY028442 (JJS), and an unrestricted grant to the Department of Ophthalmology from Research to Prevent Blindness (RPB).

Disclosure: **P. Rao**, None; **P.K. Suvas**, None; **A.D. Jerome**, None; **J.J. Steinle**, None; **S. Suvas**, None

References

1. Rowe AM, St Leger AJ, Jeon S, Dhaliwal DK, Knickelbein JE, Hendricks RL. Herpes keratitis. *Prog Retin Eye Res.* 2013;32:88–101.
2. Lobo AM, Agelidis AM, Shukla D. Pathogenesis of herpes simplex keratitis: The host cell response and ocular surface sequelae to infection and inflammation. *Ocul Surf.* 2019;17:40–49.
3. Farooq AV, Valyi-Nagy T, Shukla D. Mediators and mechanisms of herpes simplex virus entry into ocular cells. *Curr Eye Res.* 2010;35:445–450.
4. Gimenez F, Suryawanshi A, Rouse BT. Pathogenesis of herpes stromal keratitis–a focus on corneal neovascularization. *Prog Retin Eye Res.* 2013;33:1–9.
5. Thomas J, Gangappa S, Kanangat S, Rouse BT. On the essential involvement of neutrophils in the immunopathologic disease: herpetic stromal keratitis. *J Immunol.* 1997;158:1383–1391.
6. Conrady CD, Zheng M, Mandal NA, van Rooijen N, Carr DJ. IFN-alpha-driven CCL2 production recruits inflammatory monocytes to infection site in mice. *Mucosal Immunol.* 2013;6:45–55.
7. Lee DH, Ghiasi H. Roles of M1 and M2 macrophages in herpes simplex virus 1 infectivity. *J Virol.* 2017;91:1–11.
8. Niemialtowski MG, Rouse BT. Predominance of Th1 cells in ocular tissues during herpetic stromal keratitis. *J Immunol.* 1992;149:3035–3039.
9. Knickelbein JE, Hendricks RL, Charukamnoetkanok P. Management of herpes simplex virus stromal keratitis: an evidence-based review. *Surv Ophthalmol.* 2009;54:226–234.
10. Sheppard JD, Wertheimer ML, Scoper SV. Modalities to decrease stromal herpes simplex keratitis reactivation rates. *Arch Ophthalmol.* 2009;127:852–856.
11. Renfro L, Snow JS. Ocular effects of topical and systemic steroids. *Dermatol Clin.* 1992;10:505–512.
12. McGhee CN, Dean S, Danesh-Meyer H. Locally administered ocular corticosteroids: benefits and risks. *Drug Saf.* 2002;25:33–55.
13. Baxter RC. Circulating binding proteins for the insulinlike growth factors. *Trends Endocrinol Metab.* 1993;4:91–96.
14. Baxter RC. Insulin-like growth factor binding protein-3 (IGFBP-3): Novel ligands mediate unexpected functions. *J Cell Commun Signal.* 2013;7:179–189.
15. Firth SM, Baxter RC. Cellular actions of the insulin-like growth factor binding proteins. *Endocr Rev.* 2002;23:824–854.
16. Shimasaki S, Ling N. Identification and molecular characterization of insulin-like growth factor binding proteins (IGFBP-1, -2, -3, -4, -5 and -6). *Prog Growth Factor Res.* 1991;3:243–266.
17. Ranke MB. Insulin-like growth factor binding-protein-3 (IGFBP-3). *Best Pract Res Clin Endocrinol Metab.* 2015;29:701–711.
18. Hwa V, Oh Y, Rosenfeld RG. The insulin-like growth factor-binding protein (IGFBP) superfamily. *Endocr Rev.* 1999;20:761–787.
19. Clemmons DR. Insulin-like growth factor binding proteins and their role in controlling IGF actions. *Cytokine Growth Factor Rev.* 1997;8:45–62.
20. Bach LA, Headey SJ, Norton RS. IGF-binding proteins–the pieces are falling into place. *Trends Endocrinol Metab.* 2005;16:228–234.
21. Martin JL, Baxter RC. Insulin-like growth factor-binding protein from human plasma. Purification and characterization. *J Biol Chem.* 1986;261:8754–8760.
22. Baxter RC, Martin JL, Beniac VA. High molecular weight insulin-like growth factor binding protein complex. Purification and properties of the acid-labile subunit from human serum. *J Biol Chem.* 1989;264:11843–11848.
23. Yamada PM, Lee KW. Perspectives in mammalian IGFBP-3 biology: local vs. systemic action. *Am J Physiol Cell Physiol.* 2009;296:C954–976.
24. Baxter RC. Nuclear actions of insulin-like growth factor binding protein-3. *Gene.* 2015;569:7–13.
25. Jogie-Brahim S, Feldman D, Oh Y. Unraveling insulin-like growth factor binding protein-3 actions in human disease. *Endocr Rev.* 2009;30:417–437.
26. Oh Y, Muller HL, Lamson G, Rosenfeld RG. Insulin-like growth factor (IGF)-independent action of IGF-binding protein-3 in Hs578T human breast cancer cells. Cell surface binding and growth inhibition. *J Biol Chem.* 1993;268:14964–14971.
27. Robertson DM, Ho SI, Hansen BS, Petroll WM, Cavanagh HD. Insulin-like growth factor binding protein-3 expression in the human corneal epithelium. *Exp Eye Res.* 2007;85:492–501.
28. Wu YC, Buckner BR, Zhu M, Cavanagh HD, Robertson DM. Elevated IGFBP3 levels in diabetic tears: a negative regulator of IGF-1 signaling in the corneal epithelium. *Ocul Surf.* 2012;10:100–107.
29. Stuard WL, Titone R, Robertson DM. Tear levels of insulin-like growth factor binding protein 3 correlate with subbasal nerve plexus changes in patients with type 2 diabetes mellitus. *Invest Ophthalmol Vis Sci.* 2017;58:6105–6112.
30. Ning Y, Schuller AG, Bradshaw S, et al. Diminished growth and enhanced glucose metabolism in triple knockout mice containing mutations of insulin-like growth factor binding protein-3, -4, and -5. *Mol Endocrinol.* 2006;20:2173–2186.
31. Gaddipati S, Rao P, Jerome AD, Burugula BB, Gerard NP, Suvas S. Loss of neurokinin-1 receptor alters ocular surface

homeostasis and promotes an early development of herpes stromal keratitis. *J Immunol.* 2016;197:4021–4033.
32. Gaddipati S, Estrada K, Rao P, Jerome AD, Suvas S. IL-2/anti-IL-2 antibody complex treatment inhibits the development but not the progression of herpetic stromal keratitis. *J Immunol.* 2015;194:273–282.
33. Biswas PS, Rouse BT. Early events in HSV keratitis–setting the stage for a blinding disease. *Microbes Infect.* 2005;7:799–810.
34. Bryant-Hudson K, Conrady CD, Carr DJ. Type I interferon and lymphangiogenesis in the HSV-1 infected cornea - are they beneficial to the host? *Prog Retin Eye Res.* 2013;36:281–291.
35. Phillips LS, Pao CI, Villafuerte BC. Molecular regulation of insulin-like growth factor-I and its principal binding protein, IGFBP-3. *Prog Nucleic Acid Res Mol Biol.* 1998;60:195–265.
36. Albiston AL, Saffery R, Herington AC. Cloning and characterization of the promoter for the rat insulin-like growth factor-binding protein-3 gene. *Endocrinology.* 1995;136:696–704.
37. Bang P. Serum proteolysis of IGFBP-3. *Prog Growth Factor Res.* 1995;6:285–292.
38. Bang P, Brismar K, Rosenfeld RG. Increased proteolysis of insulin-like growth factor-binding protein-3 (IGFBP-3) in noninsulin-dependent diabetes mellitus serum, with elevation of a 29-kilodalton (kDa) glycosylated IGFBP-3 fragment contained in the approximately 130- to 150-kDa ternary complex. *J Clin Endocrinol Metab.* 1994;78:1119–1127.
39. Wetterau LA, Moore MG, Lee KW, Shim ML, Cohen P. Novel aspects of the insulin-like growth factor binding proteins. *Mol Genet Metab.* 1999;68:161–181.
40. Erondu NE, Dake BL, Moser DR, Lin M, Boes M, Bar RS. Regulation of endothelial IGFBP-3 synthesis and secretion by IGF-I and TGF-beta. *Growth Regul.* 1996;6:1–9.
41. Natsuizaka M, Naganuma S, Kagawa S, et al. Hypoxia induces IGFBP3 in esophageal squamous cancer cells through HIF-1alpha-mediated mRNA transcription and continuous protein synthesis. *FASEB J.* 2012;26:2620–2630.
42. Besset V, Le Magueresse-Battistoni B, Collette J, Benahmed M. Tumor necrosis factor alpha stimulates insulin-like growth factor binding protein 3 expression in cultured porcine Sertoli cells. *Endocrinology.* 1996;137:296–303.
43. Rao P, Suvas S. Development of Inflammatory Hypoxia and Prevalence of Glycolytic Metabolism in Progressing Herpes Stromal Keratitis Lesions. *J Immunol.* 2019;202:514–526.
44. Lee KW, Liu B, Ma L, et al. Cellular internalization of insulin-like growth factor binding protein-3: distinct endocytic pathways facilitate re-uptake and nuclear localization. *J Biol Chem.* 2004;279:469–476.
45. Micutkova L, Hermann M, Offterdinger M, et al. Analysis of the cellular uptake and nuclear delivery of insulin-like growth factor binding protein-3 in human osteosarcoma cells. *Int J Cancer.* 2012;130:1544–1557.
46. Lee KW, Ma L, Yan X, Liu B, Zhang XK, Cohen P. Rapid apoptosis induction by IGFBP-3 involves an insulin-like growth factor-independent nucleomitochondrial translocation of RXRalpha/Nur77. *J Biol Chem.* 2005;280:16942–16948.
47. Cobb LJ, Liu B, Lee KW, Cohen P. Phosphorylation by DNA-dependent protein kinase is critical for apoptosis induction by insulin-like growth factor binding protein-3. *Cancer Res.* 2006;66:10878–10884.
48. Coverley JA, Baxter RC. Phosphorylation of insulin-like growth factor binding proteins. *Mol Cell Endocrinol.* 1997;128:1–5.
49. Granata R, Trovato L, Garbarino G, et al. Dual effects of IGFBP-3 on endothelial cell apoptosis and survival: involvement of the sphingolipid signaling pathways. *FASEB J.* 2004;18:1456–1458.
50. Huang SS, Ling TY, Tseng WF, et al. Cellular growth inhibition by IGFBP-3 and TGF-beta1 requires LRP-1. *FASEB J.* 2003;17:2068–2081.
51. Kim KS, Kim MS, Seu YB, Chung HY, Kim JH, Kim JR. Regulation of replicative senescence by insulin-like growth factor-binding protein 3 in human umbilical vein endothelial cells. *Aging Cell.* 2007;6:535–545.
52. Baz-Martinez M, Da Silva-Alvarez S, Rodriguez E, et al. Cell senescence is an antiviral defense mechanism. *Sci Rep.* 2016;6:37007.
53. Knuever J, Willenborg S, Ding X, et al. Myeloid cell-restricted insulin/IGF-1 receptor deficiency protects against skin inflammation. *J Immunol.* 2015;195:5296–5308.
54. Kodukula P, Liu T, Rooijen NV, Jager MJ, Hendricks RL. Macrophage control of herpes simplex virus type 1 replication in the peripheral nervous system. *J Immunol.* 1999;162:2895–2905.
55. Kim JH, Choi DS, Lee OH, Oh SH, Lippman SM, Lee HY. Antiangiogenic antitumor activities of IGFBP-3 are mediated by IGF-independent suppression of Erk1/2 activation and Egr-1-mediated transcriptional events. *Blood.* 2011;118:2622–2631.
56. Oh SH, Kim WY, Lee OH, et al. Insulin-like growth factor binding protein-3 suppresses vascular endothelial growth factor expression and tumor angiogenesis in head and neck squamous cell carcinoma. *Cancer Sci.* 2012;103:1259–1266.
57. Liu B, Lee KW, Anzo M, et al. Insulin-like growth factor-binding protein-3 inhibition of prostate cancer growth involves suppression of angiogenesis. *Oncogene.* 2007;26:1811–1819.
58. Kielczewski JL, Hu P, Shaw LC, et al. Novel protective properties of IGFBP-3 result in enhanced pericyte ensheathment, reduced microglial activation, increased microglial apoptosis, and neuronal protection after ischemic retinal injury. *Am J Pathol.* 2011;178:1517–1528.
59. Kielczewski JL, Li Calzi S, Shaw LC, et al. Free insulin-like growth factor binding protein-3 (IGFBP-3) reduces retinal vascular permeability in association with a reduction of acid sphingomyelinase (ASMase). *Invest Ophthalmol Vis Sci.* 2011;52:8278–8286.
60. Kondo T, Vicent D, Suzuma K, et al. Knockout of insulin and IGF-1 receptors on vascular endothelial cells protects against retinal neovascularization. *J Clin Invest.* 2003;111:1835–1842.
61. Himpe E, Degaillier C, Coppens A, Kooijman R. Insulin-like growth factor-1 delays Fas-mediated apoptosis in human neutrophils through the phosphatidylinositol-3 kinase pathway. *J Endocrinol.* 2008;199:69–80.
62. Kooijman R, Coppens A, Hooghe-Peters E. Igf-I inhibits spontaneous apoptosis in human granulocytes. *Endocrinology.* 2002;143:1206–1212.
63. Fu YK, Arkins S, Wang BS, Kelley KW. A novel role of growth hormone and insulin-like growth factor-I. Priming neutrophils for superoxide anion secretion. *J Immunol.* 1991;146:1602–1608.
64. Walsh PT, O'Connor R. The insulin-like growth factor-I receptor is regulated by CD28 and protects activated T cells from apoptosis. *Eur J Immunol.* 2000;30:1010–1018.
65. Walsh PT, Smith LM, O'Connor R. Insulin-like growth factor-1 activates Akt and Jun N-terminal kinases (JNKs) in promoting the survival of T lymphocytes. *Immunology.* 2002;107:461–471.
66. Mohanraj L, Kim HS, Li W, et al. IGFBP-3 inhibits cytokine-induced insulin resistance and early manifestations of atherosclerosis. *PLoS One.* 2013;8:e55084.

Investigative Ophthalmology & Visual Science